Effect of Electrode Morphology on the Electrochemical Performance of Pt/YSZ Electrodes

Meng Kang, Jianjun Fang, Sufang Li[*], Tingting Liu, Congcong Wang, Ligang Tan

State Key Laboratory of Chemo/Biosensing and Chemometrics, College of Chemistry and Chemical Engineering, Hunan University, Changsha 410082, P.R. China.
[*]E-mail: hnlis@163.com

This study is focused on the effect of catalytic electrode morphology on the electrochemical performance of one of the most prominent solid state electrode systems, $Pt(O_2)/YSZ$ system. Two types of sintered $Pt(O_2)/YSZ$ electrodes (metal Pt electrode and metal-ceramic electrode) prepared by screen printing of different Pt pastes are investigated in this work. The morphology of the catalytic electrodes is characterized by scanning electron microscopy (SEM) and their electrochemical behaviors are investigated by CV techniques and chronoamperometry. Cyclic voltammetry on the Pt/YSZ catalytic electrodes evidences the characteristics of the oxygen charge exchange reaction. The corresponding redox reactions occur nearby the tripe phase boundary (tpb) and manifest themselves by one of more cathodic peaks and an anodic wave in the voltammograms. Series investigations demonstrate that the metal-ceramic electrodes show the high electrochemical activity of oxygen charge exchange reactions and can expect significant usage in the field of oxygen sensors and solid oxide fuel cells.

1. INTRODUCTION

The high temperature oxygen electrode is perhaps the most important electrode system in solid state electrochemistry, and $Pt(O_2)/YSZ$ (yttria stabilized zirconia) electrode can be viewed as a corresponding model-type material system, comparable to $Pt(O_2)/H_2O$ electrode system in aqueous electrochemistry[1]. The $Pt(O_2)/YSZ$ electrode system are commonly used for numerous applications, such as gas sensors[2], gas pumps[3], solid oxide fuel cells[4], and electrochemically promoted catalysts[5,6]. In fact, $Pt(O_2)/YSZ$ system is the most widely researched example of catalytic electrode

deposited on solid electrolyte[7-15]. Despite decades of research, a detailed understanding of the oxygen exchange mechanism and factors influencing the electrode kinetics and the electrocatalytic properties are still absent[13]，especially at high temperatures (about 773K to 1073K), which are connected with their application in the field of oxygen sensors[2,16]. Thus the systematic and knowledge-based optimization of the electrode performance and an improvement of its long-term stability require a deeper understanding of the microscopic processes of electrochemical reactions.

The most important electrochemical oxygen exchange reaction, involving the couple O_2 (g)/O^{2-}, consists of electron exchange between gaseous oxygen and O^{2-} ion of the solid electrolyte: $1/2 O_2$ (tpb) $+ 2e^- \rightarrow O_{(YSZ)}^{2-}$ (1). Considering that platinum is impermeable for oxygen, this reaction can only occur at the neighboring of the tpb (i.e. the solid electrolyte-catalyst-gas interface) because of the reaction involving reactants from all three phases [12,14,17]. As is well-known that the presence of an oxide film at the metal/electrolyte interface [18] affects the mechanism and kinetics of the electrochemical process by changing the electron properties of the metal surface and by imposing a barrier on charge transfer across the surface oxide film[17]. The existence of Pt oxide at the Pt/YSZ interface during electrochemical polarization was proposed several years ago[19,20] and assumed in recent studies[1,13,14,17]. Thus the most probable competitive electrochemically activated reaction for reaction (1) involves the PtO_x/Pt couple corresponding to the redox reaction (2)：$PtO_x + 2xe^- \rightarrow Pt + xO^{2-}$ (2). This reaction (2) involves reactants from the metal and the electrolyte phase but no reactants from the gaseous phase, so it may take place around the Pt/YSZ interface[21]. It should be emphasized that the two electrochemical reactions are not independent of each other, and the second may strongly influence the first. But to our knowledge, there is still no definite direct in situ or even ex situ experimental proof for the existence of Pt oxides in the system Pt(O_2)/YSZ during electrochemical polarization[18,21].

Among the electrochemical methods for the study of electrode processes, CV (cyclic voltammetry) plays an important role as one of the simplest and fasted methods without the requirement of expensive equipment[1]. Several papers dealing with voltammetric characterization of the Pt(O_2)/YSZ system have appeared[1,10,14,16,17,20,21], presenting on one or two cathodic peaks observed during the negative potential scan. The first peak recognized by most papers is attributed to reduction of oxygen atoms adsorbed at the tpb[15,18,21]. The second, often poorly defined, cathodic peak has also been reported in several papers[1,17,21,23,24]. Various interpretations are put forward, including either back-spillover[15,21,22], platinum oxide[1,22] or a rearranged of platinum oxide[24].

In our study, cyclic voltammetric and chronoamperometric experiments are operated to discuss the effect of the morphology on the electrochemical behavior of the Pt/YSZ electrodes. Four types of electrochemical cell equipped with distinct electrodes with different morphology have been investigated. One kind of electrode made in our lab is porous metal-ceramic electrode type, which features a high dispersion of the ceramic phase and the metal phase, corresponding to the ionic and electronic conductors. The other one is metal Pt electrode made of commercial Pt paste, which is in opposition to the porous metal-ceramic electrode in the surface character and expected to be very compact. Assuming that these morphology changes of this two types of electrodes can affect the dimensions of the reactive regions (e.g. tpb sites) and thus alter the electrochemical response[13].

The main aim of the present study is to investigate the influence of the oxygen catalytic electrode morphology on the electrochemical performance of oxygen charge transfer reactions, and move forward a single step to probe into the electrochemical performance of electrodes used in gas sensors[2,16,25] and solid oxide fuel cells[4,26].

2. EXPERIMENTAL

The electrochemical cells used in this current work consist of a three electrode system (working, reference and counter electrodes)[21,27], as shown in Fig.1, this geometry ensures a symmetrical current and potential distribution in the cell[28,29].
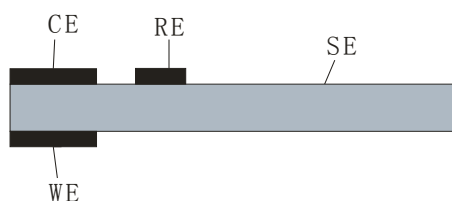
Figure 1. Electrochemical cell. WE: working electrode; CE: counter electrode;
RE: reference electrode; SE: solid electrolyte (YSZ).

The electrolyte biscuit was prepared by tape casting 8YSZ paste (8YSZ, 8 mol% yttria stabilized zirconia, purchased from Tosoh), dried at air atmosphere. The working electrodes investigated (for identification see Table1) were prepared by screen printing of different Pt pastes then the cell was sintered (preparation parameters are given in Table1). The pastes of metal-ceramic working electrode were made by ball-milling the mixture of organic material and composite platinum powders prepared by directly roasting the admixture of chloroplatinic acid, zirconium oxychloride and yttrium nitrate at 800K.. The admixture has different proportion corresponding to different electrode samples. All chemicals used in this paper were of analytical grade. The pastes of the metal Pt electrode were purchased from Kunming Institute of Precious Metals of China, which were also used as the counter and reference electrodes.

The crystallographic structure of the metal-ceramic electrode sample was characterized by X-ray diffraction (XRD, θ-2θ scans, Cu K$_{\alpha 1,2}$, Bruker D8-ADVANCE, Germany). Scanning electron microscopy (SEM, JSM-6490 LV, Japan) was used to characterize the morphology of samples. The electrochemical performance of the oxygen charge exchange reactions on the Pt(O2)/YSZ system was investigated by cyclic voltammetric and chronoamperometric experiments using an electrochemical workstation (Ingsens-3030, Smart instruments Guangzhou Co, China). The experiments were carried out at air atmosphere and atmospheric pressure, 973K. Cyclic voltammetry under continuous potential cycling between the two potential limits with different scan rate were performed. Additionally, chronoamperometry at chosen anodic potentials was carried out. The experiment results were shown in the discussion sections.

Table 1. Abbreviations for working electrodes (composed of two kinds of paste, their dimensions and the sintering parameter)

Electrode sample	Paste	Dimensions	Sintering parameter
A （Pt/YSZ)	the pure metal Pt paste	2×4 ㎜	with 1K/min to 773K, holding for 2h, 5K/min to 1273K, holding for 2h.
B (Pt/YSZ)	the pure metal Pt paste	2×4 ㎜	with 1K/min to 773K, holding for 2h, 5K/min to 1673K, holding for 2h.
C (1%YSZ-Pt/YSZ)	the metal-ceramic paste	2×4 ㎜	with 1K/min to 773K, holding for 2h, 5K/min to 1673K, holding for 2h.
D (10%YSZ-Pt/YSZ)	the metal-ceramic paste	2×4 ㎜	with 1K/min to 773K, holding for 2h, 5K/min to 1673K, holding for 2h.

3. RESULTS AND DISCUSSION

3.1. Structure characterization

The structure of the metal-ceramic electrode sample D (10%YSZ/Pt) was determined by X-ray diffraction (XRD). Fig.2 proves that ZrO_2 in the electrode displays the cubic crystal structure, in addition, the Y_2O_3 phase disappears, which manifests that the yttria partially stabilized zirconia (YSZ) phase was formed [13,18], this phase structure is beneficial to the production and transmission of oxygen ions in the overall electrode with more active reaction sites[18,30,31], which corresponding to the higher oxygen exchange reaction rate in oxygen sensors[2].
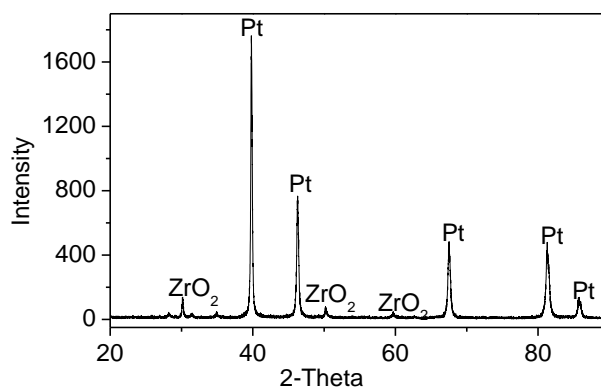
Figure 2. X-ray diffractogram of the metal-ceramic electrode sample D (10%YSZ/Pt).

3.2. Morphology characterisation

We investigated electrodes morphology before cyclic voltammetric experiments by scanning election microscopy (SEM). The Fig.3a shows that the electrode sample A (metal Pt electrode, sintered at 1273K) is virtually dense with some bubbles (red arrow in Fig.3a) after sintering. The bubbles formation is due to gas tightness. A detailed study of this phenomenon has been published previously [1,13,15]. Based on the SEM images, a poor population of tpb sites and a larger area of mental/electrolyte interface are formed. But, compared to the electrode sample A, the morphology of the other metal Pt electrode sample B (sintered at 1673K, Fig.3b) is a partly network and partly isolated platinum (blue dotted line in Fig.3b) on YSZ electrolyte. Higher temperature or longer time of sintering may motivate the coalescence mechanism and break the network, resulting in a non-conductive film formed by isolated agglomerates [17,32]. The morphology of the sample B features a higher population of tpb sites, but isolated structure of platinum on YSZ electrolyte prevents transmission of the electron in the electrode.
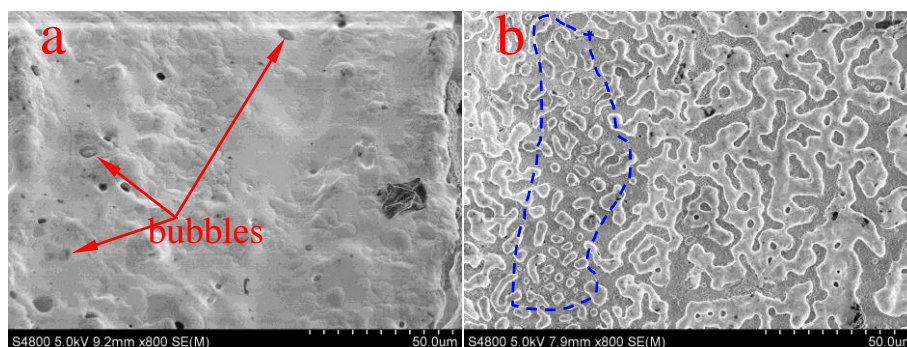
Figure 3. Representative SEM images of metal Pt electrode samples at different sintered final temperature, a: at 1273K; b: at 1673K.

Metal-ceramic electrode samples C and D are marked a porous network (shown in Fig.4), where the porosity and the microstructure depend on the preparation parameters. High sintering temperature (1673K) creates thicker bridges between particles, leading a very stable microstructure. By the backscattered electronimaging technology (BSE), metal Pt phase (the white part, red arrow in Fig.4a) displays a continuous netlike structure, which is the transmission path of electron. With the increasing percentage of YSZ phase (grey part, blue arrow in Fig.4a) in the overall electrode, the size of platinum particle becomes smaller and the dispersibility between metal Pt phase and YSZ phase is higher. This phenomenon indicates that the mixture of the YSZ phase into the metal platinum phase can effectively prevent the high temperature overgrowth and densification of platinum particles, which is in favour of the upper ambient temperature operation of the oxygen sensors.
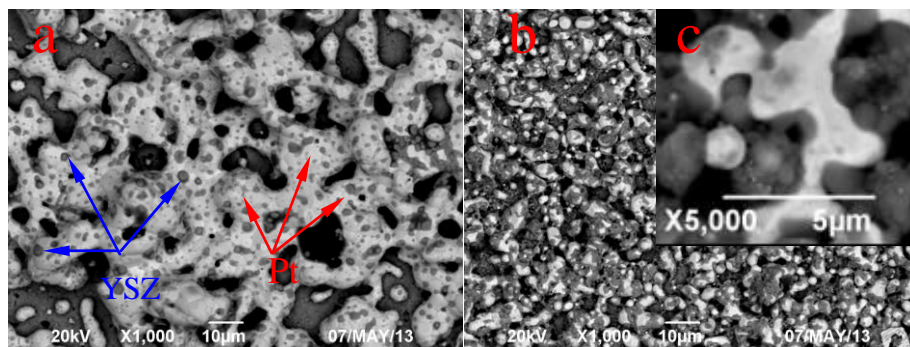
Figure 4. SEM images of metal-ceramic electrode samples C and D with different composition, a: 1%YSZ-Pt/YSZ; b: 10%YSZ-Pt/YSZ; illustration c: amplifying SEM images of sample D.

As shown in Fig.4, sample C (1%YSZ-Pt/YSZ) features continuous Pt phase without consecutive YSZ phase. The electrode of Sample C is supposed to be lower activity than sample D because of lacking YSZ phase consistency, the transmission path of O^{2-}. When the percentage of YSZ phase in the electrode reaches to 10% (sample D, corresponding to Fig.4b), electronic and ionic conductor particles with high dispersion bonds to netlike platinum phase and YSZ phase respectively and two networks intertwine together in the overall electrode. It is perfect that there is a percolation of both metal and ceramic phase in the overall electrode, the netlike platinum phase confirms the continuity of electronic conductor and continuous netlike YSZ ionic conductor allows geometric extension of tpb into volume of the electrode [17,21]. Based on these observations, sample D is expected to have a high amount of tpb sites per unit geometrical volume.

3.3 Cyclic voltammetry

3.3.1 The effect of morphology on the shape of voltammograms

In all cases a cathodic peak is observed in the voltammograms that corresponds to the reaction of oxygen chemisorbed at the tpb as described in Eq.(1)[15,18,36].

$$1/2O_{2(tpb)} + 2e- \rightarrow O(YSZ)^{2-}$$
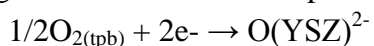
Anodic peaks that correspond to the reverse of the charge transfer reaction [35] are barely detectable in all of the voltammograms which indicates that $O_{(tpb)}$ was formed primarily from $O_{2(g)}$ and not from O^{2-}[15].

Our experiments investigated the influence of the electrode morphology on the shape of CV e.g. the directly observable difference of the metal electrode and the metal-ceramic electrode (cp.Fig.5 and Fig.7). In addition, we investigated two metal Pt electrode samples sintered at different final temperature by the cyclic voltammetry (cp. Fig.5 and Fig.6). Fig.5shows the basic voltammograms of the dense electrode (sample A, sintered at 1273K), which features a couple of cathodic and anodic peaks corresponding to the reduction and oxidation of oxygen species in the Pt(O₂)/YSZ system. The peak current is with respect to the geometrical surface area of the electrochemical reaction in the

electrode [17]. The peak current of this sample is weak compared with other samples (cp.Fig.7, Fig.7, Fig.8) because of the less tpb sites (can see Fig.3a).
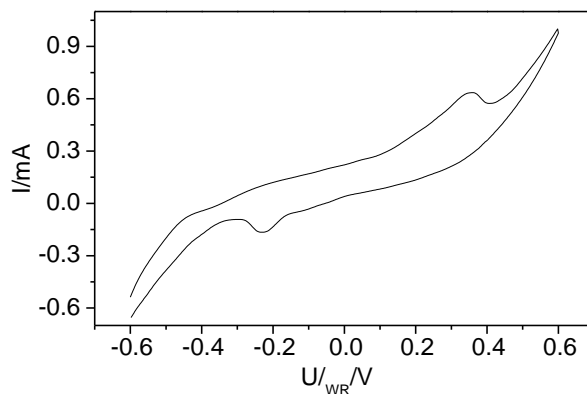
Figure 5. The basic cyclic voltammigram of the metal Pt electrode sample A. T = 973K; $v=80 mvs^{-1}$; at air atmosphere and atmospheric pressure.
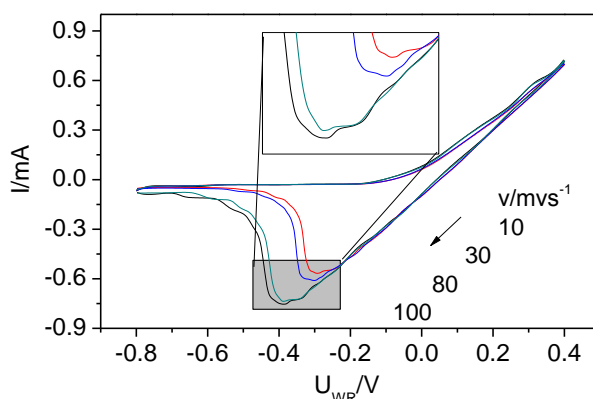
Figure 6. Effect of the scan rate v on the cyclic voltammigrams of metal Pt electrode sample B. T = 973K; at air atmosphere and atmospheric pressure.

Fig.6 shows the effect of the cycling sweep rate on the voltammogarms of the other metal electrode (sample B, sintered at 1673K). These voltammograms feature two distinct cathodic peaks and one anodic wave, which are similar to the literatures [16,17,37]. The cathodic peak current and potential are strongly dependent on the sweep rate v, the faster sweep rate, the larger cathodic peak current and the more negative peak potential. In contrast, at high cathodic potentials ($U_{WR} < -0.6V$), the current is almost sweep rate independent. The main cathodic peak corresponds to the reduction of oxygen chemisorbed at the tpb[15,18,36], and the small peak, which can overlap with the larger one , may origin from the impurities such as Si or the oxides such as PtO_x, where use of the symbol PtO_x is due to the ill-defined stoichiometry of the electrochemically formed oxide[1,14,15,17,21]. The main

peak current of sample B is five times as large as sample A because of the higher population of the tpb sites corresponding to the SEM images in Fig.3b.

When it comes to the porous metal-ceramic electrode samples, the Fig.7 shows the effect of the sweep rate on the shape of the voltammograms of the 1%YSZ-Pt/YSZ and 10%YSZ-Pt/YSZ porous metal-ceramic electrodes (sample C and D), these voltammograms show a large cathodic peak and an anodic wave, the shape of the voltammograms has a high sweep rate dependency, indicating a behavior according mostly to the oxygen charge exchange reaction such as reaction (1). The peak current of the two samples at the same sweep rate are much higher than the two metal Pt electrode samples A and B, this phenomenon is obviously due to a larger amounts of tpb sites per unit geometrical volume, as it could be expected from the different electrode dispersion seen on the SEM images Fig.3 and Fig.4. In particularly, the peak current of sample D presents twice as large as sample C at the same sweep rate, which may demonstrate more tpb sites in the metal-ceramic electrode sample D, corresponding to the geometric extension of the tpb into the volume of the electrode[17,21] because of the continuous dispersion of ionic conductor into the overall electrode. So, the high electrochemistry activity of this kind of porous metal-ceramic electrodes can expect its excellent performance in the field of oxygen sensors and solid oxide fuel cells.
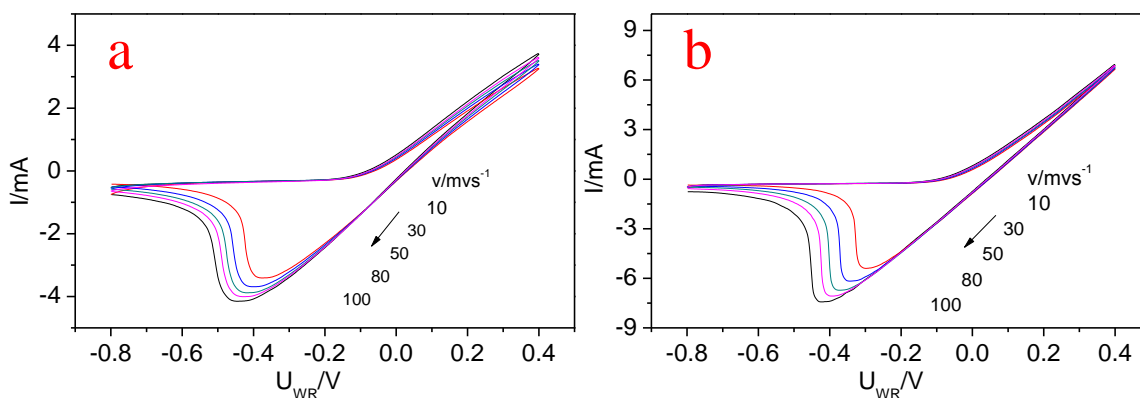
Figure 7. Effect of the scan rate ν on the cyclic voltammigrams of metal-ceramic electrode samples, a: 1%YSZ-Pt/YSZ (sampleC); b: 10%YSZ-Pt/YSZ (sample D), T = 973K, at air atmosphere and atmospheric pressure.

3.3.2 The effect of the operating temperature on the shape of voltammograms

We investigated the effect of the operating temperature on the shape of cyclic voltammograms of the electrode sample D. Fig.8 shows the voltammograms of the four different temperatures. As we can see, with the increasing of operating temperature, the cathodic peak area becomes more and more big, and so as the peak current, which corresponds to the high activity of the oxygen sensors at high operating temperature.
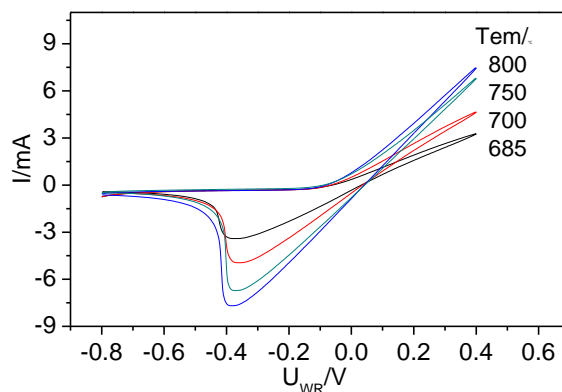
Figure 8. Effect of the operating temperature on the cyclic voltammigrams of the metal-ceramic electrode sample D, v=80 mvs^{-1}, at air atmosphere and atmospheric pressure.

3.3.3 The effect of the anodic reversal potential $U_{r,a}$ on the shape of voltammograms.

Specific to the electrode sample D, we researched the influence of different anodic reversal potential on the peak features and cycling behavior at 973K and 80mvs^{-1}. Fig.9 shows that each of the voltammograms qualitatively reveals the same feature: one clear cathodic peak and one visible wave along the positive scan. The chosen potential range apparently has a great impact on the voltammograms, the greater anodic reversal potentials, the bigger cathodic peak area and the more negative peak potential. The systematic variation of the anodic reversal potential also offers the possibility to obtain information on corresponding electrochemistry processes of oxygen charge exchange reaction and its reversal reaction [15,18]: the anodic wave corresponds to the main cathodic peak.
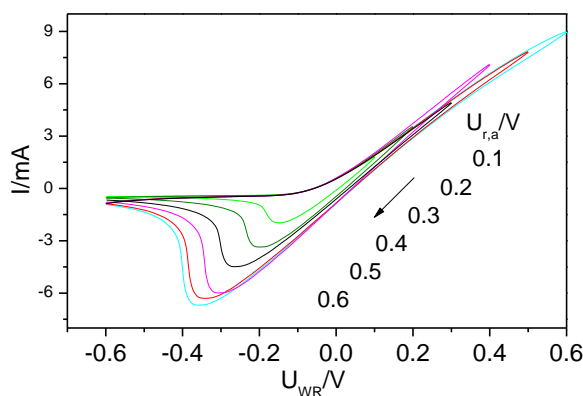
Figure 9. Effect of the anodic reversal potential $U_{r,a}$ on the cyclic voltammigram of the metal-ceramic electrode sample D. v=80 mvs-1, T = 973K, at air atmosphere and atmospheric pressure.

3.4 Chronoamperometry

Then, we investigated the chronoamperometry of the four electrode samples in order to study the evolution of current with time under potentiostatic polarization as a method to complement the cyclic voltammetric data[17,21] and explore the system stability of the four electrodes. A pretreatment was performed during 300s at U_{WR}=-0.8V before measuring each curve, which aimed to reduce all the probable oxide and to reach a identical initial state, After the pretreatment, the potential was immediately changed to a chosen anodic potential, and the current was measured as a function of time. The obtained chronoamperometric curves in Fig.10a show that the four samples present high system stability of electrochemical reactions and the sample D obviously has highest catalytic activity than other samples, which is most probably due to the ideal morphology (can see Fig.4b) of the continuous dispersion of ionic conductor into the overall electrode.

Fig.10b shows the effect of the anodic potential U_{WR} on the chronoamperometric curves of the electrode sample D. The value of the initial current (t = 0s) increases with U_{WR}. A fast current drop is observed at very short time (t < 20s), with the development of time (20s< t <100s), the falling tendency of the current is observed in Fig.10b. At long times (t > 100s), the current of all curves are rather stable and present high reaction activity, which indicate a persistent electrochemistry oxygen charge exchange reaction in this Pt(O2)/YSZ system, corresponding to the system stability of oxygen sensors. This porous metal-ceramic electrode can be expected a wonderful application in the field of oxygen sensors and solid oxide fuel cells in the future.
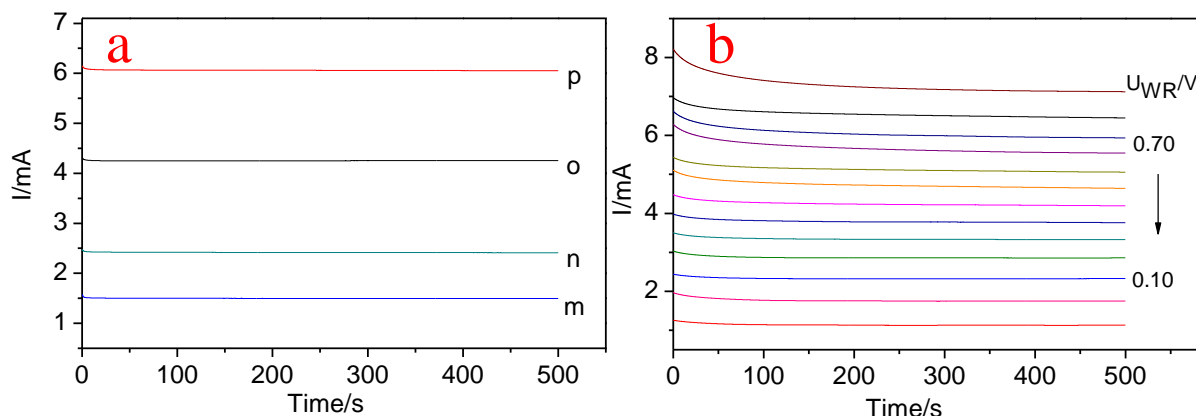
Figure 10. a: The chronoamperometric curves of four electrode samples (m: sample A; n: sample B; o: sample C; p: sample D). U_{WR}=0.60V. b: Effect of the anodic potential U_{WR} on the chronoamperometric curves of the metal-ceramic electrode sample D. T = 973K; at air atmosphere and atmospheric pressure.

4. CONCLUSIONS

The relationship among preparation of Pt/YSZ electrodes, their corresponding morphology and electrochemical measurements in air atmosphere is discussed in this work, the following is the conclusion:

Typical Pt(O2)/YSZ characteristics such as cathodic peaks and the anodic wave are obviously observed with all the electrode samples, corresponding to the reduction and oxidation of oxygen species in the Pt(O_2)/YSZ system.

The electrode morphology of the Pt/YSZ system influences the shape of voltammograms, either by changing the value of the current or by the appearance of peaks.

The amount of tpb impacts the value of peak current, which dues to the electrode morphology changes.

The results of cyclic voltammetric and chronoamperometric experiments demonstrate that porous metal-ceramic electrodes have an excellent electrochemistry performance corresponding to the usage of oxygen sensors.

Finally, we conclude that our present understanding of electrode electrochemistry process in solid state is still in its infancy. We believe that major advances in solid state electrochemistry will be possible if future studies concentrate on high quality (model-type) sample preparations[37] and combining electrochemical measurements with spectroscopic and microscopic in situ techniques[13,38].

References

1. E. Mutoro, B. Luerben, S. Guther, J. Janek, *Solid State Ionics*, 180 (2009) 1019-1033.
2. L.R. Skubal and M.C. Vogt, *Proc.SPIE–Int. Soc.Optical Eng*, 5586 (2004) 45.
3. T. Hibino, Y. Kuwahara, T. Otsuka, N. Ishida and T. Oshima, *Solid State Ionics*, 107 (1998) 217.
4. K.V. Kordesch, J.C.T.De Olivera, Ullmann's, Encyclopedia of Industrial Chemistry, vol. A12, VCH, New York, 1989.
5. C.G. Vayenas, S. Bebelis, C. Pliangos, S. Brosda and D. Tsiplakides, Electrochemical Activation of Catalysis: Promotion, Electrochemical Promotion, and Metal-Support Interactions, Kluwer Academic/Plenum Publishers, New York, 2001.
6. A. Katsaounis, Z. Nikopoulou, X.E. Verykios, and C.G. Vanas, *Journal of Catalysis*, 222 (2004) 192-206.
7. J. Sasaki, J. Mizusaki, S. Yamauchi and K. Fueki, *Solid State Ionics*, 3–4 (1981) 531.
8. J. Mizusaki, K. Amano, S. Yamauchi and K. Fueki, *Solid State Ionics*, 22 (1987) 323.
9. A. Mitterdorfer and L.J. Gauckler, *Solid State Ionics*, 117 (1999)187.
10. M. Goge, K. Heggestad and M. Gouet, *Solid State Ionics*, 18–19(1986) 1228.
11. K. Schindler, D. Schmeisser, U. Vohrer, H.D. Wiemhofer and W. Gopel, *Sens. Actuators*, 17 (1989) 555.
12. B. Luerssen, J. Janek and R. Imbihl, *Solid State Ionics*, 141–142 (2001) 701.
13. H. Popke, E. Mutoro, B. Luerben, J. Janek, *Solid State Ionics*, 189 (2011) 56-62.
14. Eva Mutoro, Nils Baumann, and Jurgen Janek. *The Journal of Physical Chemistry Letters*, 2010.1.2322-2326.
15. Mas Rahayu Jalil, Naimah Ibrahim, Danai Poulidi, Ian S.Metcalfe, *Solid State Ionics*, 225 (2012) 390-394.
16. E.L. Shoemaker, M.C. Vogt, F.L. Dudek, *Solid State Ionics*, 92 (1996) 285-292.

17. A. Jaccoud, G. Foti, R. Wuthrich, H. Jotterand, and CH. Comninellis, *Topics in Catalysis* Vol, 44, No. 3, June 2007.
18. H. Popke, E. Mutoro, B. Luerben, J. Janek, *Catalysis Today*, 202 (2013) 12-19.
19. T. Chao, K.J. Walsh, P.S. Fedkiw, *Solid State Ionics*, 47 (1991) 277.
20. T. Kenjo, Y. Yamakoshi, K. Wada, *J. Electrochem. Soc*,140 (1993) 2151.
21. Arnaud Jaccoud, Gyorgy Foti, Christos Comninellis, *Electrochimica Acta*, 51 (2006) 1264-1273.
22. J. Yi, A. Kaloyannis and C.G. Vayenas, *Electrochim. Acta*, 38 (1993) 2533.
23. Cyril Falgairette, Gyorgy Foti, *Catalysis Today*, 146 (2009) 274-278.
24. Tsaofang Chao, K.J. Walsh and P.S. Fedkiw, *Solid State Ionics*, 47 (1991) 277.
25. Takao Murase and T. Yoshimura, Pat. Nr. 5130002, Method of processing oxygen concentration sensor by applying AC current, and the thus processed sensor, 1992.
26. A. Barbucci, R. Bozzo, G. Cerisola and P. Costamagna, *Electrochim. Acta*, 47 (2002) 2183.
27. D. Poulidi, I. Metcalfe, *J. Appl. Electrochem*, 38 (8) (2008) 1121.
28. G. Foti, V. Stankovic, I. Bolzonella and Ch. Comninellis, *J. Electroanal. Chem*, 532 (2002) 191.
29. L. Bultel, C. Roux, E. Siebert, P. Vernoux, F. Gaillard, *Solid State Ionics*, 166 (2004) 183-189.
30. J. Nielsen, T. Jacobsen, *Solid State Ionics*, 178 (2007) 1001-1009.
31. Seetharaman Sridhar, Victor Stancovski, Uday B. Pal, *Solid State Ionics*, 100 (1997) 17-22
32. B. El Roustom, G. Foti and Ch. Comninellis, *Electrochem. Comm*, 7 (2005) 398.
33. E. Mutoro, B. Luerßen, S. Günther, J. Janek, *Solid State Ionics*, 179 (2008) 1414.
34. E. Mutoro, S. Günther, B. Luerßen, I. Valov, J. Janek, *Solid State Ionics*, 179 (2008) 1835.
35. S. Pizzini, M. Bianchi, P. Colombo and S. Torchio, *J. Appl. Electrochem*, 3 (1973) 153.
36. C.G. Vayenas, A. Ioannides, S. Bebelis, *J. Catal*, 129 (1) (1991) 67.
37. G. Beck, H. Fischer, E. Mutoro, V. Srot, K. Petrikowski, E. Tchernychova, M. Wuttig, M. Rühle, B. Luerßen, J. Janek, *Solid State Ionics*, 178 (2007) 327.
38. J. Janek, B. Luerßen, E. Mutoro, H. Fischer, Sebastian Günther, *Topics in Catalysis*, 44 (2007) 399.